An Efficient Simulation Technique for High-Frequency Piezoelectric Inertia Motors

Matthias Hunstig, Tobias Hemsel, Walter Sextro
University of Paderborn
Pohlweg 47 - 49, 33098 Paderborn, Germany

***Abstract*—Piezoelectric inertia motors use the inertia of a body to drive it by means of a friction contact in a series of small steps. These motors can operate in "stick-slip" or "slip-slip" mode, with the fundamental frequency of the driving signal ranging from several Hertz to more than 100 kHz. To predict the motor characteristics, a Coulomb friction model is sufficient in many cases, but numerical simulation requires microscopic time steps. This contribution proposes a much faster simulation technique using one evaluation per period of the excitation signal. The proposed technique produces results very close to those of time-step simulation for ultrasonics inertia motors and allows direct determination of the steady-state velocity of an inertia motor from the motion profile of the driving part. Thus it is a useful simulation technique which can be applied in both analysis and design of inertia motors, especially for parameter studies and optimisation.**

I. Introduction

Piezoelectric inertia motors, originally developed for fine positioning applications in the laboratory [1], [2], [3], have been applied in several fields in the last years, often in miniaturised consumer goods [4], [5], [6], [7], [8] because these motors have a simple construction and are controlled by a single signal, which allows for low production costs and simplifies miniaturisation.

Inertia motors use the inertia of a body to drive it by means of a friction contact in a series of small steps. These motors are also known as "stick-slip drives" because the steps are classically regarded to be composed of a phase of static friction between the driving and the driven part and a phase where the two parts slide on each other. But inertia motors can successfully operate also without phases of static friction, which is known as the "slip-slip" mode. Fig. 1 illustrates this mode of operation.

Slip-slip operation has been gaining wider recognition in the last years and some authors [8], [9], [10] have described inertia motors operating in both stick-slip and slip-slip mode. The authors of this contribution have recently investigated the principle advantages, disadvantages und limitations of these two modes of operation [11], [12], [13]. It was found that the velocity reachable in stick-slip operation is limited principally, while slip-slip operation allows much higher velocities with suitable driving signals.

In the first years of inertia motor development linear sawtooth driving signals are dominant, but the ideal driving signal for maximum velocity produces a parabolic extension of the actuator followed by an extremely fast contraction [12], [14]

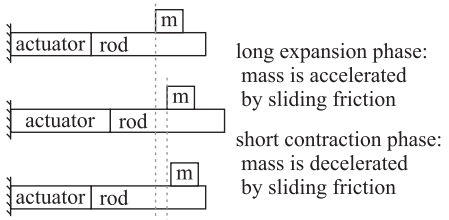

Figure 1. Schematic showing one period of a simple inertia motor operating in "slip-slip" mode

("parabolic sawtooth"). Newer developments use rectangular voltage signals producing sawtooth-like displacement signals due to the dynamics of the actuator [6], [15], [16], or a superposition of two sinusoidal signals using resonance amplification [10], [17], [18], [19] to form a frequency-limited sawtooth approximation [11], [13].

The fundamental frequency of the driving signals for inertia motors ranges from several Hertz to more than 100 kHz depending on the motor design. Especially motors using resonance effects are mostly driven at ultrasonic frequencies and use sliding friction for propulsion.

In many cases, a Coulomb friction model is sufficient for describing the dynamic behaviour of such motors [20]. But exact numerical simulation with this simple model requires appropriate methods and very small time steps, especially if stiction is to be considered, and is thus computationally expensive. This contribution proposes a simulation technique on a macroscopic time-scale which is much faster than classical microscopic time-scale simulation, shows no instabilities, and additionally allows direct calculation of the steady-state motor velocity without simulation of the transient behaviour.

II. Efficient Simulation Technique

Figure 2 shows a rigid body model of a simple inertia motor without the piezoelectric actuator. A slider of mass m_s hangs below a driving rod with the inclination angle γ. The contact force F_c between rod and slider results from the gravitational force F_g and an external force F_M. This force and an additional force F_x act on the center of gravity C of the slider. The friction force $F_f(t)$ acts between rod and slider, $x_R(t)$ and $x_S(t)$ are the displacements of the two parts. This model serves as an example for the following considerations.

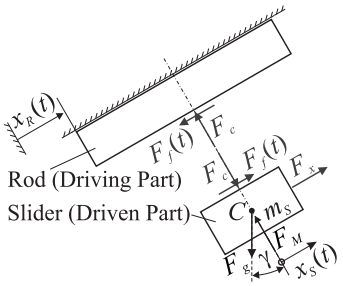

Figure 2. Rigid body model of a translational inertia motor

A. Prerequisites and Definitions

The driving part of an inertia motor generally shows a periodic motion signal. In many cases, especially in motors designed for high velocity operation which are driven with high frequency signals, the absolute value of the driving part acceleration $\ddot{x}_R(t)$ is almost always larger than the absolute value of the corresponding break-away acceleration. This is the acceleration above which the parts would start to slide if they were sticking to each other before, which means that there are no phases of stiction with significant length, the motors operate in slip-slip mode. As an example, fig. 3 shows a typical acceleration profile.

As there is no phase of stiction, the velocities of driving and driven part are equal only for infinitely short moments. Two times are defined: t_p^+ is the time in period p during which $\dot{x}_R(t) > \dot{x}_S(t)$, i. e. the driving part has a higher velocity than the driven part. $t_p^- = T - t_p^+$ is the time in period p during which $\dot{x}_R(t) < \dot{x}_S(t)$, i. e. the driving part has a lower velocity than the driven part, where T is the period of the driving signal.

Assuming Coulomb friction, the friction force can only take two values in slip-slip mode. Thus, the acceleration of the driven part is either a_d^+ or a_d^-:

$$a_d^+ = \ddot{x}_S(\dot{x}_R > \dot{x}_S) = -g\sin(\gamma) + \frac{\mu_d F_c}{m_S} + \frac{F_x}{m_S} \quad (1)$$

$$a_d^- = \ddot{x}_S(\dot{x}_R < \dot{x}_S) = -g\sin(\gamma) - \frac{\mu_d F_c}{m_S} + \frac{F_x}{m_S} \quad (2)$$

Over one period, the total velocity change of the driven part is then described by

$$\Delta\bar{v}_{S,p} = a_d^+ \cdot t_p^+ + a_d^- \cdot t_p^-. \quad (3)$$

Fig. 4 shows typical velocity signals for driving and driven part over one period T. Compared to the quickly changing velocity of the driving part with a fluctuation amplitude of $\hat{v}_R$, the fluctuation $\hat{v}_S$ of the velocity of the driven part is small. Thus, the velocity of the driven part can be regarded constant over one period. With this constant $\bar{v}_S$, the values t_p^+ and t_p^- depend only on the slider velocity at the beginning of period p, which equals the end of period $p-1$. This allows to define a characteristic function $t^+(\bar{v}_S)$ which is described by

$$t^+(\bar{v}_S) = \frac{1}{2} + \frac{1}{2T}\int_0^T \operatorname{sgn}\left(\dot{x}_R(t) - \bar{v}_S\right) \mathrm{d}t. \quad (4)$$

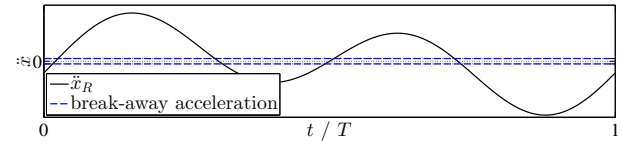

Figure 3. Typical acceleration $\ddot{x}_R(t)$ of the driving part over one period T of the excitation signal.

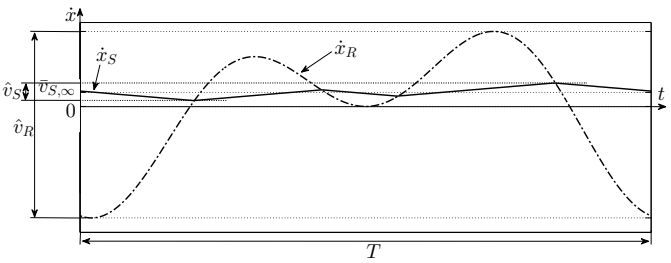

Figure 4. Typical velocities of driving ($\dot{x}_R$) and driven part ($\dot{x}_S$) over one period T in steady state.

From this definition follows:

$$t^+\left(\bar{v}_S > \max\left(\dot{x}_R(t)\right)\right) = 0 \quad (5)$$

$$t^+\left(\bar{v}_S < \min\left(\dot{x}_R(t)\right)\right) = 1 \quad (6)$$

If there is no interval $[t_1, t_2]$, with $t_1 < t_2$, in which the velocity of the driving part $\dot{x}_R(t)$ is constant, $t^+(\bar{v}_S)$ is strictly decreasing and invertible for $\min\left(\dot{x}_R(t)\right) \leq \bar{v}_S \leq \max\left(\dot{x}_R(t)\right)$. In high-frequency inertia motors, the driving part is constantly in motion and unless large external forces act on the driven part, it cannot reach higher velocities than the driving part. The inverse function $\bar{v}_S\left(t^+\right)$ is thus defined for any normally operating high-frequency inertia motor.

B. Period-Wise Simulation

With the assumptions discussed above, the change of the mean velocity of the driven part in period p, $\Delta\bar{v}_{S,p} = \bar{v}_{S,p} - \bar{v}_{S,p-1}$, can be calculated as

$$\Delta\bar{v}_{S,p} = a_d^+ \cdot t_p^+(\bar{v}_{S,p-1}) + a_d^- \cdot t_p^-(\bar{v}_{S,p-1}) \quad (7)$$

where $\bar{v}_{S,p}$ is the mean velocity of the slider in period p. The velocity in any period can thus be calculated sequentially if the driving frequency $1/T$, the starting velocity $\bar{v}_{S,0}$, and the characteristic function $t^+(\bar{v}_S)$ of the driving part motion are known, using

$$\bar{v}_{S,p} = \bar{v}_{S,p-1} + \Delta\bar{v}_{S,p}. \quad (8)$$

C. Direct Calculation of the Steady-State Velocity

High-velocity inertia motors usually require more than one period to reach their steady state velocity $\bar{v}_{S,\infty}$, if they operate with a continuously moving slider in slip-slip mode they approach this velocity asymptotically [12], [13]. The steady state velocity can easily be determined using the quantities

introduced above: In steady state, the velocity does not change, thus $\Delta\bar{v}_{S,\infty} = 0$. From (7) follows for this case:

$$t_\infty^+ = \frac{a_d^-}{a_d^- - a_d^+} T \tag{9}$$

Using $\bar{v}_S(t^+)$, $\bar{v}_{S,\infty}$ can be determined directly if the excitation signal, a_d^-, and a_d^+ are known.

D. Implementation

The proposed simulation technique has been implemented in MATLAB. The given excitation signal $\dot{x}_R(t)$ is analysed to determine the characteristic function $t^+(\bar{v}_S)$: For $n_{\bar{v}_S}$ equally distributed velocities $\bar{v}_S$ between $\min(\dot{x}_R(t))$ and $\max(\dot{x}_R(t))$, the fraction of the signal period during which $\dot{x}(t) > \bar{v}_S$ is calculated. The obtained values of t^+/T are stored in a table together with the corresponding velocity. For period-wise simulation of the motor motion, the value of t^+/T corresponding to the slider velocity at the beginning of a period is determined from the stored table using linear interpolation. A second option is to calculate the exact value of $t_p^+(\bar{v}_S)$ for each period directly from the excitation signal without using a lookup table. This option is faster if a small number of periods is simulated. In both cases, the velocity at the end of each period is calculated using (7) and (8) and then used to calculate the velocity change in the next period.

To directly determine the steady state velocity of the motor, t_∞^+ is determined using (9) and the corresponding velocity is determined from the stored table using linear interpolation.

E. Validation and Discussion

In order to validate the proposed simulation technique, it is first applied to a motor build for fundamental investigations of friction and inertia motor control in the authors' lab. This motor can be driven with arbitrary signals at frequencies up to some kilohertz. For this investigation, a signal with a fundamental frequency of 1575 Hz is used with a peak to peak displacement of the driving part of 25 µm. This signal has been obtained by approximating a parabolic sawtooth signal with a limited number of harmonics [13], [11]. The motor is simulated using time-step simulation with and without stiction and using the proposed period-wise technique with parameters identified in previous experiments [21]: $m_S = 1.4\,\mathrm{g}$, $\gamma = 0°$, $F_c = 1\,\mathrm{N}$, $F_x = 0\,\mathrm{N}$, $\mu_d = 0.16$, $\mu_s = 0.176$. All period-wise simulations are done with $n_{\bar{v}_S} = 1024$. The average velocity signal used for determining $t^+(\bar{v}_S)$ was calculated over periods 51 to 100, neclecting the first periods after start-up to exclude transient effects.

The results shown in Fig. 5 show that there is a significant difference between time-step simulation with and without stiction. This indicates that the first prerequisite for period-wise simulation – slip-slip operation – is not fulfilled. This is also one reason why there is a significant difference between time-step and period-wise simulation.

Equation (3) shows that in any motor with given a_d^+ and a_d^-, increasing the frequency linearly decreases the velocity change per period, as $T = t_p^+ + t_p^-$ decreases. If the velocity profile of the driving part is unchanged, the same relation is true for the oscillation amplitude $\hat{v}_S$ of the velocity of the driven part. An approximately constant velocity of the driven part is the second prerequisite for period-wise simulation, so a higher frequency generally leads to a better fit between time-step and period-wise simulation. In order to validate this statement for higher frequencies, three different ultrasonic inertia motors recently presented in literature are simulated:

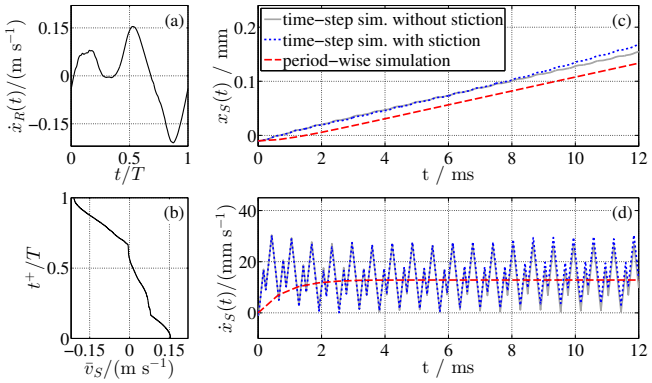

Figure 5. Time-step and period-wise simulation of an inertia motor operated at $1/T = 1575\,\mathrm{Hz}$: (a) Measured average velocity $\dot{x}_R(t)$ of the driving part over one period, (b) Characteristic function $t^+(\bar{v}_S)/T$, (c) Simulated displacement $x_S(t)$, and (d) Simulated velocity $\dot{x}_S(t)$ of the driven part.

1) A motor by Nishimura et al. [10] using a Langevin transducer driven with two superimposed sine voltages at 21.6 and 43.2 kHz with a peak to peak displacement of the driving part of about 28 µm.
2) The translational degree of freedom of a motor by Tuncdemir et al. [16] driven with a square wave voltage signal at 58.8 kHz with a peak to peak displacement of the driving part of about 0.55 µm.
3) A miniature motor by Morita et al. [18] driven with two superimposed sine voltages at 288.0 and 576.0 kHz with a peak to peak displacement of the driving part of about 0.45 µm.

The velocity signals of the driving parts are digitised from figures in the referred publications, the average velocity signal is then calculated over as many periods as possible from the published measurements. Values required for the simulation are taken from the referred publication if possible, otherwise the values are approximated on the basis of the published motor design and performance.

The simulation results documented in fig. 6 show that even though the motors are driven with different frequencies and amplitudes and show very different steady state velocities and acceleration phases, the proposed period-wise simulation technique and time-step simulation produce very similar results for each motor. The acceleration phase is reproduced almost perfectly and the calculated steady-state velocities differ by less than 1 %. The gain in simulation speed highly depends on the algorithm used for time-step simulation. With $n_{\bar{v}_S} = 1024$, period-wise simulation in its current implementation is more than three times faster than a very simple fixed-step algorithm

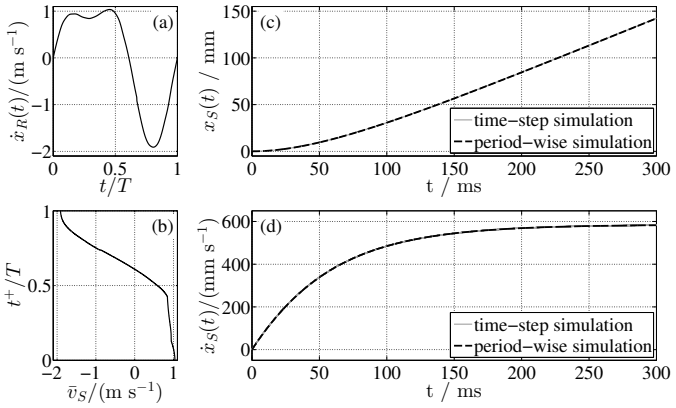

1) Motor by Nishimura et al. [10] – given parameters: $1/T = 21.6\,\text{kHz}$, $F_c = 1.52\,\text{N}$, $\gamma = 0$; chosen parameters: $m_s = 5\,\text{g}$, $F_x = 0\,\text{N}$, $\mu_d = 0.15$ (steel-alumina)

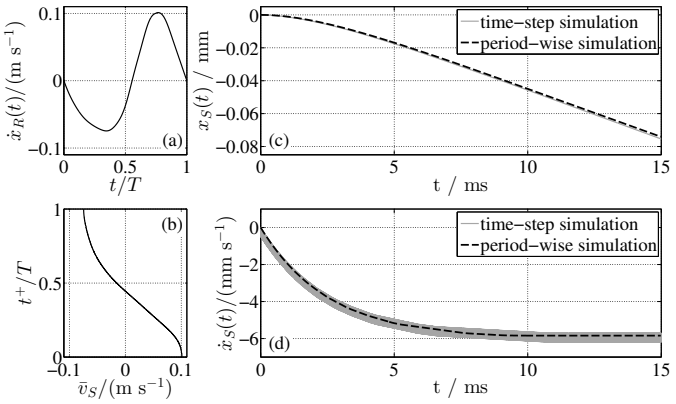

2) Motor by Tuncdemir et al. [16] – given parameters: $1/T = 58.8\,\text{kHz}$, $F_x = 4\,\text{mN}$, $\gamma = 0$; chosen parameters: $m_s = 1\,\text{g}$, $F_c = 1\,\text{N}$, $\mu_d = 0.2$ (brass-plastic)

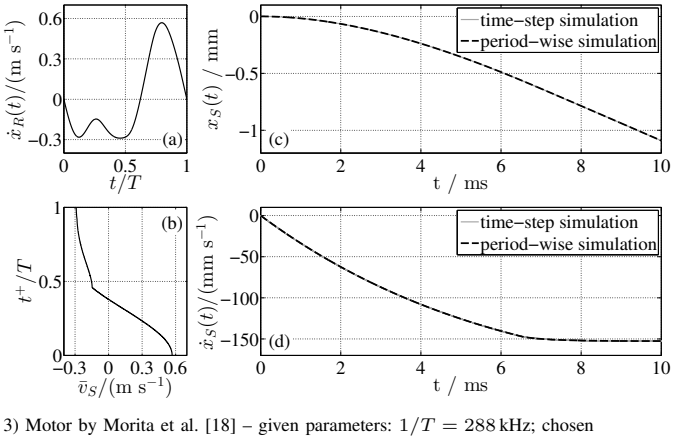

3) Motor by Morita et al. [18] – given parameters: $1/T = 288\,\text{kHz}$; chosen parameters: $F_x = 0\,\text{N}$, $\gamma = 0$, $m_s = 1\,\text{g}$, $F_c = 1\,\text{N}$, $\mu_d = 0.15$ (steel-steel)

Figure 6. Time-step and period-wise simulations of three ultrasonic inertia motors: (a) Average velocity $\dot{x}_R(t)$ of the driving part over one period, (b) Characteristic function $t^+(\bar{v}_S)/T$, (c) Simulated displacement $x_S(t)$, and (d) Simulated velocity $\dot{x}_S(t)$ of the driven part.

with 1024 points per period and much faster than any sophisticated algorithms considering stiction.

III. Conclusions

Compared to classic time-step simulation, the proposed period-wise simulation technique allows significantly faster simulation of high-frequency inertia motors without any significant loss of accuracy. This makes it a useful simulation technique for analysis, design, and optimisation of inertia motors. The possibility to determine the steady-state velocity from the motion profile of the driving part directly is very useful for parameter studies and for comparison and optimisation of excitation signals. The characteristic function used in period-wise simulation is also easy to implement with a lookup table for microcontrollers, for example for velocity control of inertia motors in low-cost applications.

References

[1] M. Anders, M. Thaer, and C. Heiden, "Simple micropositioning devices for STM," *Surf. Sci.*, vol. 181, no. 1-2, pp. 176–182, Mar. 1987.

[2] T. Higuchi, Y. Hojjat, and M. Wanatabe, "Micro actuators using recoil of an ejected mass," in *Proceedings of the IEEE Micro Robots and Teleoperators Workshop*. Hyannis, Massachusetts: IEEE, 1987.

[3] D. W. Pohl, "Dynamic piezoelectric translation devices," *Rev. Sci. Instrum.*, vol. 58, no. 1, pp. 54–57, Jan. 1987.

[4] K. Matsusaka, S. Ozawa, R. Yoshida, T. Yuasa, and Y. Souma, "Ultra-compact optical zoom lens for mobile phone," in *Proceedings of SPIE-IS&T Electronic Imaging*, vol. 6502, Feb. 2007, p. 650203 (10 pp.).

[5] K. Uchino, "Piezoelectric motors for camera modules," in *ACTUATOR 2008 Conference Proceedings*, Bremen, Jun. 2008, pp. 157–160.

[6] D. Paik, K. Yoo, C. Kang, B. Cho, S. Nam, and S. Yoon, "Multilayer piezoelectric linear ultrasonic motor for camera module," *J. Electroceram.*, vol. 22, no. 1, pp. 346–351, Feb. 2009.

[7] D. A. Henderson, "US patent 8059346: Linear drive systems and methods thereof," Nov. 2011.

[8] J. Lee, W. S. Kwon, K. Kim, and S. Kim, "A novel smooth impact drive mechanism actuation method with dual-slider for a compact zoom lens system," *Rev. Sci. Instrum.*, vol. 82, p. 085105, 2011.

[9] Y. Okamoto and R. Yoshida, "Development of linear actuators using piezoelectric elements," *Electronics and Communications in Japan, Part 3*, vol. 81, no. 11, pp. 11–17, 1998.

[10] T. Nishimura, H. Hosaka, and T. Morita, "Resonant-type smooth impact drive mechanism (SIDM) actuator using a bolt-clamped langevin transducer," *Ultrasonics*, vol. 52, no. 1, pp. 75–80, 2012.

[11] M. Hunstig, T. Hemsel, and W. Sextro, "Analysis of different operation modes for inertia motors," in *ACTUATOR 2012 Conference Proceedings*, Bremen, 2012, pp. 761–764.

[12] M. Hunstig, T. Hemsel, and W. Sextro, "Stick-slip and slip-slip operation of piezoelectric inertia drives – part I: Ideal excitation," *Sens. Actuators, A*, 2012, submitted (Ms. Ref. No. SNA-D-12-00603R1).

[13] M. Hunstig, T. Hemsel, and W. Sextro, "Stick-slip and slip-slip operation of piezoelectric inertia drives – part II: Frequency-limited excitation," *Sens. Actuators, A*, 2012, submitted (Ms. Ref. No. SNA-D-12-00604).

[14] M. Hunstig and T. Hemsel, "Drive signals for maximizing the velocity of piezoelectric inertia motors," *J. Korean Phys. Soc.*, vol. 57, no. 41, pp. 938–941, Oct. 2010.

[15] B. Koc, "Piezoelectric motor, operates by exciting multiple harmonics of a square plate," in *ACTUATOR 2010 Conference Proceedings*, Bremen, 2010, pp. 194–197.

[16] S. Tuncdemir, S. O. Ural, B. Koc, and K. Uchino, "Design of translation rotary ultrasonic motor with slanted piezoelectric ceramics," *Jpn. J. Appl. Phys.*, vol. 50, no. 2, p. 027301, Feb. 2011.

[17] R. Bansevicius and V. Blechertas, "Multi-degree-of-freedom ultrasonic motors for mass-consumer devices," *J. Electroceram.*, vol. 20, no. 3, pp. 221–224, 2008.

[18] T. Morita, H. Murakami, T. Yokose, and H. Hosaka, "A miniaturized resonant-type smooth impact drive mechanism actuator," *Sens. Actuators, A*, vol. 178, pp. 188–192, May 2012.

[19] M. Suzuki, H. Hosaka, and T. Morita, "Resonant-type smooth impact drive mechanism actuator with two langevin transducers," *Advanced Robotics*, vol. 26, no. 3-4, pp. 277–290, 2012.

[20] F. Altpeter, "Friction modeling, identification and compensation," Ph.D. dissertation, EPFL, Lausanne, Jun. 1999.

[21] M. Hunstig, T. Hemsel, and W. Sextro, "Modelling the friction contact in an inertia motor," *J. Intell. Mater. Syst. Struct.*, 2012, submitted (manuscript ID JIM-11-376.R2).